Assessment of soil redistribution rates in a Mediterranean olive orchard in South Spain using two approaches: $^{239+240}$Pu and soil erosion modelling

Vanesa García-Gamero [a,*], J.L. Mas [b], Andrés Peñuela [a], Santiago Hurtado [c], Adolfo Peña [d], Tom Vanwalleghem [a]

[a] Department of Agronomy, University of Córdoba, Da Vinci building, Madrid km 396 Rd., 14071 Córdoba, Spain
[b] Department of Applied Physics I, Universidad de Sevilla, ETSII, Sevilla, Spain
[c] Department of Applied Physics II, Universidad de Sevilla, ETSA, Sevilla, Spain
[d] Department of Rural Engineering, Civil Constructions and Engineering Projects, University of Córdoba, Da Vinci building, Madrid km 396 Rd., 14071 Córdoba, Spain

ARTICLE INFO

Keywords:
Soil erosion
Plutonium isotopes
WaTEM/SEDEM
Cultivated land
Mediterranean agroecosystems

ABSTRACT

Soil redistribution by water and tillage soil erosion has a profound effect on the spatial variability of soil security indicators. In this study, we assess the potential of estimating long-term soil redistribution rates across a Mediterranean olive orchard catchment using two methods: $^{239+240}$Pu and the WaTEM/SEDEM model. Additionally, we identify potential sources of uncertainty explain result discrepancies, and offer guidance for reducing uncertainty. Soil sampling points were taken both in the inter-row areas and below the tree canopies and $^{239+240}$Pu inventories were converted into soil redistribution rates using MODERN. Sediment yield data measured in the catchment outlet is used to calibrate WaTEM/SEDEM. The results show a poor agreement between both methods. In this sense, these results indicate that both methods are considerably affected by several sources of uncertainty, both inherent to the methods themselves and related to the specific conditions of the study area. The latter are mainly related to anthropogenic changes in the soil surface related to soil tillage and rill filling practices and an important past land leveling effect. Despite the discrepancies, both methods convey a similar overarching message: soil security and olive production can be highly threatened in the Mediterranean in the next decades. This study demonstrates the potential advantages of combining FRN-based estimates and model simulations and highlights the importance of selecting an appropriate study area in this type of studies and the need to recognize associated uncertainties when estimating soil redistribution rates, whether employing FRN-based or modelling methods.

1. Introduction

Soil security plays an important role in food security, water security, energy security, climate change abatement, biodiversity protection, and ecosystem service delivery (McBratney et al., 2014). It is at the core of the EU Green Deal (Panagos et al., 2022) and the new EU soil strategy which aims to achieve healthy soils by 2050, with concrete actions by 2030. In Europe, and in particular, the Mediterranean region with a long and varied history of human-induced soil erosion and agricultural land management, reconstructing past soil erosion is essential both to identify the main factors threatening soil security and define effective mitigation measures (Durán et al., 2009; Gómez et al., 2009, 2014a). Determining soil loss rates that encompass at least several decades can provide a better insight into long-term trends and the relative importance of climate and land management impacts.

The use of radionuclides has the potential to estimate long-term soil erosion rates. However, the most used radionuclide, cesium (^{137}Cs) is losing its utility because of its short half-life ($T_{1/2} = 30.2$ yr) leading to decreasing environmental concentrations (Percich et al., 2022). Consequently, the use of longer-life radionuclides is becoming increasingly important. Plutonium (Pu) is present in the Northern Hemisphere environment due to past nuclear weapon testing, with the most abundant isotopes being ^{239}Pu ($T_{1/2} = 24110$ yr) and ^{240}Pu ($T_{1/2} = 6563$ yr). Pu radionuclides ($^{239+240}$Pu) have been tested and validated relative to other "traditional" radionuclides (e.g., ^{137}Cs and ^{210}Pbex) for deriving soil erosion rates under various upland agro-environments that have been carried out in Germany (Schimmack et al., 2002, 2001), Switzerland (Alewell et al., 2014; Zollinger et al., 2015), Australia (Hoo

* Corresponding author at: Department of Agronomy, University of Córdoba, Da Vinci building, Madrid km 396 Rd., 14071 Córdoba, Spain.
E-mail address: g02gagav@uco.es (V. García-Gamero).

https://doi.org/10.1016/j.catena.2024.108052
Received 7 September 2023; Received in revised form 8 April 2024; Accepted 16 April 2024
Available online 25 April 2024
0341-8162/

et al., 2011; Lal et al., 2013), Northeast China (Xu et al., 2013; Zhang et al., 2016) and South Korea (Meusburger et al., 2016). Alewell et al. (2017) reviewed previous studies and listed the following advantages of using Pu: (i) Unlike other radionuclides, Pu inventories are not significantly affected by nuclear power plant accidents like Chernobyl, except in the immediate vicinity, leading to a more homogeneous spatial distribution, (ii) the long half-lives of Pu make it suitable for use in future studies over the next several decades, (iii) they have higher applicability than other radionuclides such as $^{210}Pb_{ex}$ because of their low concentration in soils, (iv) they have the analytical advantage of higher accuracy as compared to $^{210}Pb_{ex}$ (Iurian et al., 2015). On this matter, Peñuela et al.(2023) found that Pu isotopes and $^{210}Pb_{xs}$ can provide more accurate and reliable results compared to traditional indicators such as ^{137}Cs. Moreover, Pu offers a higher sample throughput if inductively coupled plasma mass spectrometry (ICP-MS) techniques are applied. This method solves the analytical difficulties that have limited the use of Pu for dating recent sediments (Ketterer et al., 2002), who highlighted Pu isotopes have all the needed prerequisites and advantages to become one of the next anthropogenic soil radiotracers of importance to determine soil security under climate change and land use changes.

Although radionuclides allow us to estimate long-term and spatially distributed soil erosion rates, this method has limitations. FRN-based estimations are usually unvalidated and uncertain (Parsons and Foster, 2011) and the conversion of FRN inventories into erosion rates is a source of substantial uncertainty (Walling and He, 1998), as well as the interpolation methods used to spatialize point estimations. Moreover, it is not possible to unveil the contribution of specific erosion processes, water or tillage erosion, from these single values. Soil redistribution by tillage or any other mechanical force on soils, besides water erosion, needs to be considered as they potentially dominate soil redistribution patterns (Wilken et al., 2020). For this purpose, we need additional sources of information, such as soil erosion models.

Previous studies combining radionuclide (mainly ^{137}Cs) and modelling approaches generally use radionuclide estimations to calibrate (Lizaga Villuendas et al., 2022; Porto et al., 2013; Quijano et al., 2016), validate (Walling et al., 2003) or both calibrate and validate (Porto et al., 2010; Walling and He, 2002) the models applied, assuming that radionuclide estimations are accurate. However, we should not forget that not only models but FRN-based estimations can be highly uncertain (Batista et al., 2019). Therefore, the use of FRN-based estimations for calibration purposes, rather than reducing uncertainty, may just propagate it into the model.

An alternative approach is to combine different independent methods (Meusburger et al., 2014), in particular FRN-based estimations and model simulations. In previous studies, FRN-derived rates of soil erosion typically exhibit poor agreement with model estimates (Bacchi et al., 2003; Belyaev et al., 2005; He and Walling, 2003; Lacoste et al., 2014; Martinez et al., 2009; Warren et al., 2005) but it is unclear whether it stems from errors in FRN-based techniques or limitations in the modeling process (Batista et al., 2019). Nevertheless, by critically comparing the results of FRN-based and modelling methods we can gain valuable insights and guide future improvements (Martinez et al., 2009; Batista et al., 2019). In particular, this comparison can serve as a form of cross-validation. If the two methods consistently show similar trends and magnitudes, it increases confidence in the accuracy of the estimates. Conversely, if they show discrepancies, it can highlight areas of uncertainty or potential issues in either approach. This acknowledges uncertainty and can guide further refinement of the methods. With this comparison, we can also capture different aspects and scales of the soil erosion process. Models can represent the interannual variability of soil erosion processes while radionuclides multidecadal trends in soil erosion. In addition, the use of a model permits the discrimination of the contribution of water and tillage erosion. Finally, even if both methods show important discrepancies in the results but yield similar conclusions, for instance, that past and current soil loss rates are unsustainable, we can then enhance confidence in the reliability of this overall message.

To the best of our knowledge, no study has compared soil redistribution estimates from $^{239+240}Pu$ and soil erosion modelling, and in particular, no study has used $^{239+240}Pu$ estimates to unveil soil redistribution rates in cultivated soils in Andalusia (southern Spain). In Andalusia, soil erosion is one of the major threats to soil security, particularly in olive orchards because of the hilly terrain where they are mainly cultivated without vegetation cover (Gómez et al.,2014a). This is the largest olive-growing region worldwide with olive orchards covering 19 % of the region's surface (Ministerio de Agricultura Pesca y Alimentación, 2022). Therefore, there are a significant number of studies assessing erosion under this crop (Gómez-Limón et al., 2012). Based on official data 52.7 % of the olive orchard surface suffers high (>12 t ha^{-1} yr^{-1}) to very high soil erosion (>100 t ha^{-1} yr^{-1}) in this region (Junta de Andalucía, 2022).

Specifically, the objectives of this study are (i) to assess long-term soil redistribution rates estimated from two methods: $^{239+240}Pu$ and soil erosion modelling, (ii) to identify and gain insights into discrepancies between the results of both methods and their associated uncertainties, (iii) to guide to reduce these uncertainties and (iv) to assess how soil security will evolve until the end of the 21st century and throughout the 22nd century in the study area.

2. Materials and methods

2.1. Study area

The study area is an olive orchard "*La Conchuela*" (37°49′04.6″N 4°53′45.6″W) (Córdoba, southwestern Spain) (Fig. 1), with a surface of 8 ha. The climate in the area is Mediterranean. The average annual rainfall is 655 mm with 77 % of rain concentrated in the autumn months, i.e., October-March. The average air temperature is 17.5 °C (Gómez et al., 2023). The dominant soil types belong to the Typic Haploxeret subgroup of the Soil Taxonomy (Soil survey staff, 2022) or Vertisol according to the FAO classification (Gómez et al., 2009). Catchment elevation ranges from 122 to 163 m. a. s. l. and its average slope is 10 %. The field was selected because it is representative of olive orchards in Andalusia (conventional tillage and high erosion rates) and because of data availability reasons: sediment yield measured data from 2006 to 2011 necessary for the model calibration, data of past agricultural practices, and well-documented soil descriptions. From 1963 to 1993, cereals were grown in the study area. The tillage systems consisted of a scarifier with a working depth up to 27 mm, a disc harrow for post-harvest treatment to incorporate plant residue into the soil, another scarifier labor with a working depth up to 22 mm, and a rake. Soil fertilization and seeding. The seeder usually buried the fertilizer. The current olive trees were planted at 6 × 7 m spacing in 1993, which replaced the original cereal crop. Until 2008, surface tillage was performed with a disc harrow at a working depth up to 10 or 15 cm. Occasionally a subsoiler was also used at a depth of 50–60 cm to improve the drainage of the soil. Afterward, soil management consisted of spontaneous vegetation controlled by mowing and applying glyphosate, occasionally.

The crop change from cereal to an olive orchard in the study area involved land leveling which was performed before the orchard implantation to prevent temporary waterlogging in clay soils. This land leveling consisted of removing soil from the tree lanes, approximately a 0.05 m thick layer, to form ridges on which olive trees were grown (Fig. 2). It resulted in a roughly additional soil loss of 16 t ha^{-1} yr^{-1} in the inter-row area and, consequently, an additional soil deposition rate of 40 t ha^{-1} yr^{-1} on the ridge. It is estimated a net difference of 56 t ha^{-1} yr^{-1} between inter-row (indicated with a location icon and letter X in Fig. 2) and below-canopy sampling sites (indicated with a location icon and letter C in Fig. 2). While these estimates are based on field observations of the current topography, they are considered highly uncertain because of the lack of quantitative information or records of the survey data to validate these estimates.

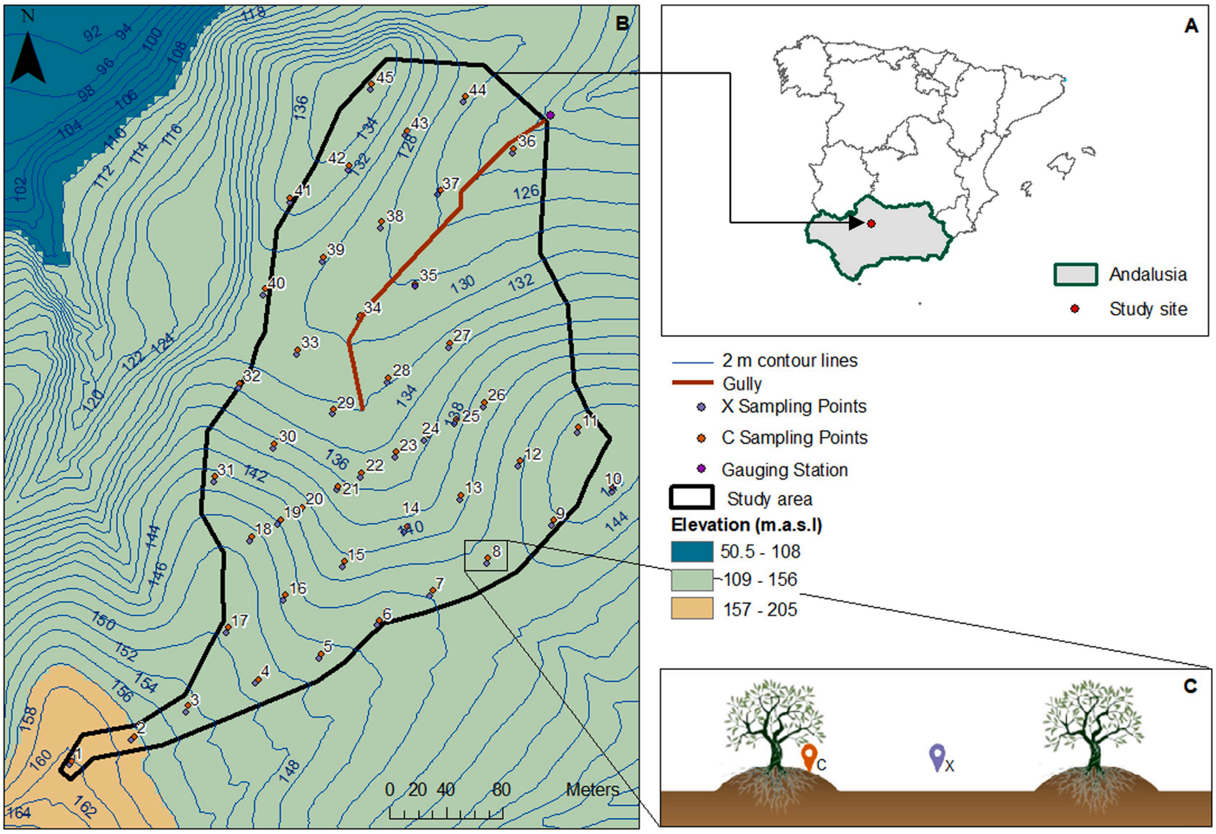

Fig. 1. Description of the study area: A. The study site (dot in red) is located in southwestern Andalusia, Spain (grey area); B. Topography of the study area with 2 m contour lines (blue lines), sampling points, gauging station and gully location; C. Schematic diagram of ridge and furrow in "La Conchuela" olive orchard and location where samples were taken, both below-canopy (C) and inter-row (X).

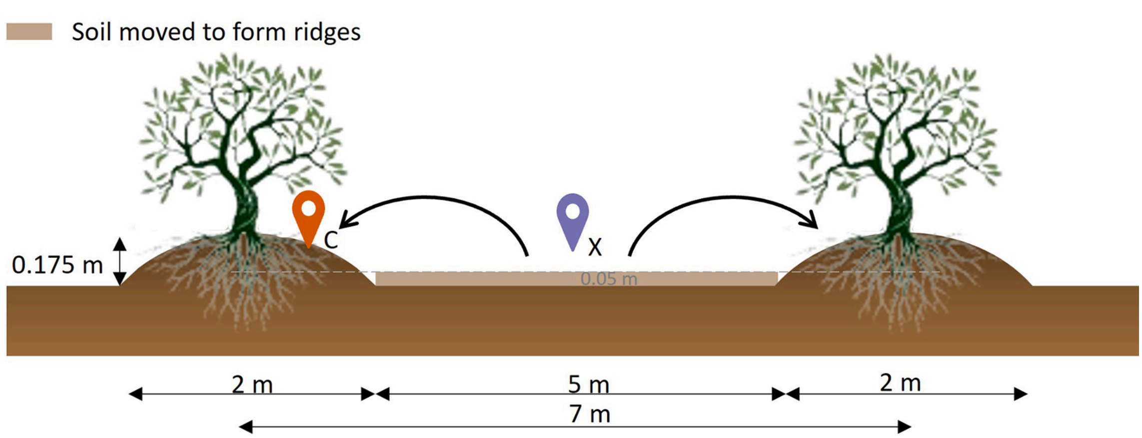

Fig. 2. Schematic diagram of ridge and furrow in "La Conchuela" olive orchard performed in 1993. Ridges to plant the olive trees were formed using a layer of soil approximately 0.05 m thick from the inter-row area. Sampling location below-canopy (C) and in the inter-row (X).

2.2. Soil sampling

Soil sampling took place in 2010, a total of 83 soil profiles (41 along the inter-row and 42 below the canopy) were collected in different transects across the olive orchard (Gómez et al., 2023) (Fig. 1). Sampling depth intervals were 0–5, 5–10, 15–20, 0–30, 30–60 and 60–90 cm. Each interval slice was thoroughly mixed during the pretreatment to generate a composite layer. For the sake of clarity, it is important to note that 90 soil profiles were initially performed equally distributed in the inter-row and below canopy. However, at the time of analysis of these samples, 2023, there was no soil sample availability at the following seven points: X1, X23, X24, X34, C23, C24, and C34 (Fig. 1).

Three reference soil cores were collected at the reference site from the vertices of a triangle 0.5 m side length, down to a depth of 0.90 m at 0.05 m intervals. Each of the 0.05 m slices was thoroughly mixed during the pretreatment to generate a composite 0.05 m layer for each interval. The reference location was located 1.5 km from the study catchment, in a nearby field on a flat surface. This area was ploughed, but given its flat topography, we can consider that no effective soil loss or gain has taken place (Govers et al.,1999; Lobb, 2006).

In addition, a reference soil profile was analyzed with a full soil profile pit. This soil profile was dug near sampling point X26, in a flat area at the top of the hillslope. A full soil profile description was made following the guidelines of USDA-NRCS (Schoeneberger et al., 2012). The soil profile description can be seen in Table 1 in the Supplementary Material.

2.3. Conversion of $^{239+240}$Pu inventories to soil redistribution rates

For Pu analysis, composite samples of the 0–30 and 30–60 cm were used when available. For those cases where just the 0–30 cm layer was available just the upper layer was used.

ICP-MS was used for the analysis of Pu isotopes by application of a methodology developed by Ketterer et al. (2002) and subsequently adapted as described by Peñuela et al. (2023). In brief, plutonium was extracted from soil ashes by leaching, and after filtration of the leachate and adjusting the Pu oxidation state, it was extracted by using TEVA® extraction chromatography. This method provides detection limits in the range of 5–10 mBq kg^{-1} for 10–15 g of soil ashes (Peñuela et al., 2023). One out of each five samples was used as quality control samples consisting of replicate sample preparation and measurements, blank samples (sandstone samples isolated from radioactive fallout), and the analysis of several aliquots of CRM samples (IAEA-384). Pu contents in this material are much higher than the Pu concentrations we expected in the fallout-level samples; hence every IAEA-384 aliquot was diluted into sandstone (1:350 m:m). The samples were measured at the University of Seville Research, Technology, and Innovation Centre (CITIUS) using an Agilent 8800 ICP-MS/MS coupled to a CETAC ARIDUS II nebulizer. All the quality control samples resulted in values within the expected ones. The MODERN model (Arata et al., 2016a, 2016b) estimates erosion or deposition rates based on the comparison (in the original reference, "alignment") of the total fallout radionuclide (FRN) inventory at the sampling site and its depth profile at reference site; in this way, the model returns a solution as a thickness of the soil layer affected by erosion or deposition. The main assumption is that the depth distribution of the selected FRN is the same at the reference and the sampling sites, as could be expected for any situation where FRN-based models could be applied. Among the main features of MODERN are that its application does not require a transect sampling approach and, additionally, it does not make any assumption on the shape of the radionuclides profile. The soil redistribution rates are estimated for the 1963–2010 period, i.e., the time of maximum nuclear fallout to the year of soil sampling. For MODERN calculations the different sampling depths used (30 or 60 cm) were taken into account. An additional MODERN advantage is the fact that it is not required that the reference profile and the sampling points have the same depth; the only requirement is that the sampling point depth is less than or equal to that of the reference profile.

As described by Arata et al. (2016b), MODERN might not reach convergence under certain conditions: 1) when the sampling sites contain inventories less than that found in the last measured layer of the depth profile. This situation could be expected for certain sampling sites when the net erosion rates are high. To prevent this situation, we used the function "addSmoothedLayers", which allows incorporating at the end of the soil profile a certain number of simulated layers. Their values are derived from an exponentially decreased fitting based on a certain number of experimental values, in this case, the last three layers of the experimental reference profile. 2) When sampling sites show inventories higher than the reference profile for a certain sampling depth (i.e., deposition sites). To prevent this, the function "addDepositionLayers" was used. This function allows adding on top of the soil core a certain number of hypothetical sediment layers which would be transferred and deposited from an upslope topsoil horizon. Our data show that this addition does not affect the results obtained for eroded sites. In this case, we added two layers of topsoil with an average of the top 10 cm, which would be representative of the thorough mixing of the deposited sediment during the transport and deposition processes.

The $^{239+240}$Pu-based point estimates of soil redistribution rates were geostatiscally interpolated (using inverse distance weighted) to obtain a gridded spatial representation that matches the spatial resolution of the WaTEM/SEDEM model (5 m × 5 m), facilitating a meaningful comparison. Moreover, we evaluated the correlation between the interpolated $^{239+240}$Pu-based map and different topographical variables: slope gradient, profile curvature, and slope length and slope gradient factor (LS factor), to identify the dominant erosion process. Profile curvature, which represents the concavity or convexity of the land surface, can influence the vulnerability of a slope to tillage erosion. Convex landforms are generally more susceptible to tillage erosion. Hence, a strong correlation between profile curvature and soil erosion rates can suggest that tillage erosion is predominant. Conversely, a strong correlation with the LS factor, i.e. flow accumulation area, might indicate that water erosion is predominant.

2.4. WaTEM/SEDEM model

The WaTEM/SEDEM model estimates long-term mean annual net soil erosion rates using an empirical spatially distributed sediment delivery model (Verstraeten et al., 2002). The water erosion component is based on the Revised Universal Soil Loss Equation (RUSLE; Renard et al., 1991). Sediment transport by overland runoff is modeled according to a transport capacity equation (TC, t ha^{-1} yr^{-1}):

$$TC = k_{tc}RK(LS - 4.1S_g^{0.8}) \quad (1)$$

where k_{tc} (m) comprises the transport capacity coefficient, R, K, and LS are RUSLE factors and Sg (m/m) is the slope gradient. Sediment deposition occurs when the transport capacity of the raster cell is smaller than the amount of sediment reaching it; otherwise, sediment is redistributed downslope (Verstraeten et al., 2007).

Tillage erosion refers to the downslope transport of soil because of plowing. Tillage transport coefficient (k_{till}) determines the intensity of tillage erosion, and net flux because tillage is proportional to the slope gradient along a hillslope of infinitesimal length (Govers et al., 1999):

$$Q_{s,t} = k_{till}S_g \quad (2)$$

where $Q_{s,t}$ represents the net downslope flux due to tillage translocation (kg m^{-1} yr^{-1}), k_{till} is the tillage transport coefficient (kg m^{-1} yr^{-1}), and S_g is the local slope gradient (m/m).

The transport capacity parameters k_{till} and k_{tc} depend on the land cover and are site-specific. Therefore, they need to be calibrated based on local data for each implementation of the model.

Table 1
Parametrisation of the WaTEM/SEDEM model.

Parameter	Value	Unit	Source
RUSLE factors			
P	1.0	–	Standard value for soil management without support practices
C	C_{cereal}:0.14 $C_{oliveorchard}$:0.3	–	From soil management following Gómez et al. (2003); Panagos et al. (2015b)
R	850	MJ mm ha^{-1}h^{-1} yr^{-1}	From available source for the location following ICONA (1988)
K	0.035	Mg h MJ^{-1} mm^{-1}	From soil data following Gómez et al. (2003)
LS	Variable	–	Calculated using 5 m DEM provided by the Spanish National Geographic Institute
Tillage transport coefficient			
k_{till}	600	kg m^{-1}	Vanwalleghem et al. (2011)
Transport capacity coefficient varied during the calibration			
k_{tc}	5–3000*	m	

* n = 23.

2.5. Model inputs

The main input data required to run WaTEM/SEDEM are the Digital elevation model (DEM) of the study area and the parameters of the RUSLE model (Table 1). The DEM, derived from LiDAR data, with a resolution of 5 m, and the parcel shape were supplied in the form of IDRISI GIS (Clark Labs Inc.). The transport capacity coefficient, k_{tc}, was fitted using measured sediment yield data, as indicated in the following section.

For the study period (1963–2010), soil erosion was weighted averaged according to the years destined for each crop, 30 years cereal and 17 years olive orchard, following:

$$\frac{30\,yr\cdot Erosion_{cereal}+17yr\cdot Erosion_{olive\ orchard}}{47\,yr}, \tag{3}$$

where $Erosion_{cereal}$ and $Erosion_{oliveorchard}$ are the soil redistribution rates calculated for the period of cereal land use (30 years) and for the period of olive orchard use (17 years), respectively, using their corresponding C-factor (Table 1).

2.6. Model calibration

The WaTEM/SEDEM model implementation in agricultural landscapes requires the calibration of the transport capacity coefficient (k_{tc}). The higher the k_{tc}, the more sediment can be transported downslope. The k_{tc} coefficient is dependent on land use: lower for well-vegetated surfaces such as forest, grassland, and pasture, and higher for poorly vegetated surfaces.

The original model was calibrated using observed data on sediment yield from 21 catchments for a resolution of 20 by 20 m in Belgium (Verstraeten et al., 2002). We used sediment yield data measured at the outlet of the study catchment for five years (2006–2011) by Gómez et al. (2014b). The sediment yield was measured using a gauging station equipped with an automatic rain gauge and a sediment sampler. The sediment sampler used a filter with a 1 mm screen mesh to capture the total suspended sediment load. Runoff samples were collected after every storm, and the samples were oven-dried to determine the instantaneous sediment concentration. This concentration was then used in conjunction with the associated instantaneous discharge throughout the runoff hydrograph to calculate the total soil loss from a runoff event.

The calibration process consisted of a systematic sampling of the parameter k_{tc} at discrete steps, ranging from 5 to 3000 (Table 1). For each value of the parameter, annual sediment yield (t) was computed for the catchment. This allowed a comparison of the measured and predicted values. Besides average weather conditions, it is advisable to ensure that the model calibration period covers a diverse spectrum of conditions, ranging from exceptionally high to exceptionally low precipitation periods (Daggupati et al., 2015; Mai, 2023; Zheng et al., 2018). This recommendation is fulfilled by the presence of both a dry year (2008–2009) and a wet year (2009–2010) within the 5-year calibration period. It must be noted that for each year of the calibration we used the R-factor estimated by Gómez et al. (2014b). This approach is similar to previous WaTEM/SEDEM studies, and we even use a longer calibration period than most of them (Table 2). As pointed out by Peeters et al. (2008), models calibrated with sediment yield data over short-term periods can still successfully simulate longer-term erosion rates provided that erosion data are correctly interpreted and integrated with a model that adequately describes the main processes observed. In Peeters et al. (2008), a 3-year calibration of the WaTEM LT model in Ganspoel (Belgium) was found to be successful in simulating long-term erosion patterns and rates derived from soil profile truncation studies.

Table 2
Temporal extent of sediment yield data used for the WaTEM/SEDEM model calibration in different studies.

Location	Temporal extent (yr)	Source
Hammeveld (Bertem, Belgium)	3	Vandaele & Poesen, 1995
Balaton basin (Hungary)	9	Jordan et al., 2005
Ganspoel (Huldenberg, Belgium)	3	Peeters et al., 2008
Barasona Reservoir (Central Spanish Pyrenees)	3	Alatorre et al., 2010
Guizhou Plateau (SW China)	3	Luo et al., 2021

The Nash-Sutcliffe model efficiency (NSE; Nash and Sutcliffe, 1970) was used for assessing the goodness of fit of the model results according to the following equation:

$$NSE = 1-\frac{\sum_{i=1}^{n}(O_i-P_i)^2}{\sum_{i=1}^{n}(O_i-O_{mean})^2} \tag{4}$$

where O_i is the observed value, P_i is the predicted value, O_{mean} is the mean observed value and n is the number of observations ($n = 5$). NSE can range from $-\infty$ to 1, and represents the initial variance accounted for in the model. The closer the value to 1, the more efficient is the model whereas $NSE < 0$ indicates that the observed mean is a better predictor than NS model efficiency. The statistical analysis and data management were performed using the R Software (version 4.2.3)(R Core Team, 2023).

3. Results and discussions

3.1. Assessment of $^{239+240}Pu$ soil redistribution rates

The reference profile is shown in Fig. 3, being Pu activity concentrations above the limit of detection of the technique at high depths (90 cm depth). This finding is not surprising bearing in mind that 1) ^{137}Cs can be detected in Andalusian Mediterranean soils even at depths of 55–60 cm (Mabit et al., 2012), 2) it has been shown that Pu migrates deeper than Cs in the Mediterranean soils (Guillén et al., 2015), and 3) using 15 g of soil sample per analysis (when available) allows decreasing the limit of detection of the technique. On the other hand, using similar techniques (ICP-MS) other authors detected Pu isotopes at remarkable depths. For instance, Ketterer et al. (2004) detected Pu isotopes at the deeper part of a 50 cm soil core in Colorado, USA; Raab et al. (2018) detected them at 70 cm depth in soils from the Sila Massif uplands (Italy), and Zhang et al. (2019) did it even at the maximum soil core focus (80 cm) in soil samples from the Loess Plateau in China.

The value of $^{239+240}Pu$ activity concentrations in the study site showed high spatial variability (CV = 40.3 %) ranging from 15.1 mBq kg^{-1} to 127 mBq kg^{-1} with a mean value of 59.1 ± 23.8 mBq kg^{-1}. Similarly, the $^{239+240}Pu$ inventories also varied from 10.6 to 68.5 Bq m^{-2} (CV = 41 %) with a mean value of 33.3 ± 13.6 Bq m^{-2}. The results are similar to those found by Peñuela et al. (2023) in a nearby study area in the Hornachuelos Natural Park in southern Spain, ranging from 1.9 to 60.6 Bq m^{-2}.

The $^{239+240}Pu$ reference inventory for the study site was 52.9 Bq m^{-2}. In the reference soil profile, the $^{239+240}Pu$ was concentrated not only in the upper soil layers but roughly homogeneous down to 0.55 m indicating that the soil was ploughed (Fig. 3). As mentioned above, surface tillage was performed at a working depth up to 10 or 15 cm but occasionally, a subsoiler was used at a depth of 50–60 cm to improve the drainage of the soil.

As much as 88 % of the sampling points in the study site had inventories lower than the reference inventory indicating a predominance of $^{239+240}Pu$ loss. In 10 sampling points, $^{239+240}Pu$ inventories exceeded the value from the reference site indicating that these sampling points have experienced soil deposition. The 60–90 cm depth layer was tested in 19 of the sampling points, all of them being soil erosion points, finding values systematically below the limit of detection of the technique. This is expected given that at uneroded positions locations (reference cores), 87 % of the Pu inventory was concentrated in the upper 60 cm.

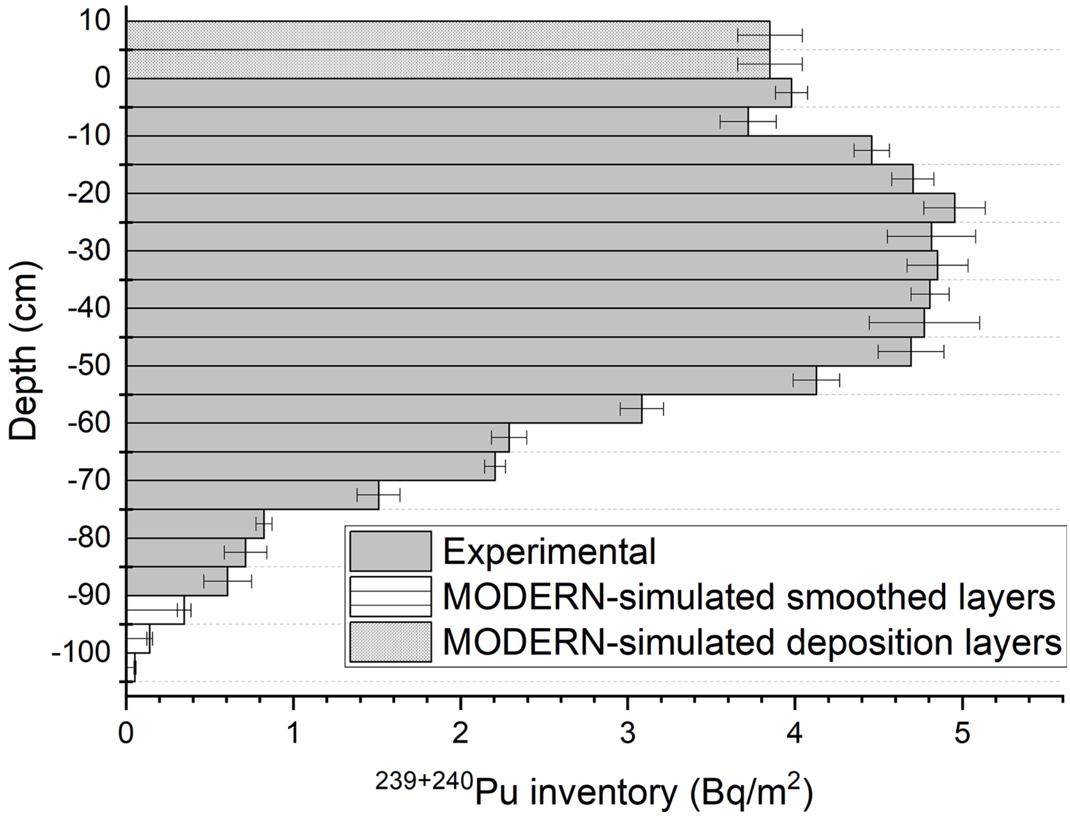

Fig. 3. Depth distribution of $^{239+240}$Pu inventory profile at the reference site. The profile shows the layers added by simulation on top of the core for the characterization of deposition sites and at the bottom of the core for the characterization of sampling sites with inventories below the lowest experimental values. Please find details in the text. Error bars correspond to the quadratic expansion of all the sources of experimental uncertainty.

Individually, the distribution for the $^{239+240}$Pu inventories for inter-row (X) and below-canopy (C) points is shown in Fig. 4. The former group had its peak around 25–30 Bq m^{-2}, whereas the latter peaked at around 30–35 Bq m^{-2}. The distribution of $^{239+240}$Pu inventories for inter-row (X) points is shifted to the left relative to the distribution of $^{239+240}$Pu inventories for below-canopy (C) points. This indicates that a greater number of points located in the inter-row area show higher soil erosion rates than those located below-canopy. This is mainly because we compare inter-row points subject to water and tillage erosion with those below-canopy only subject to water erosion.

The calculated $^{239+240}$Pu soil redistribution rates show a 95 % Confidence Interval (CI) [−85.4, −54.2] t ha^{-1} yr^{-1} for the inter-row points (X) (Fig. 5 A) and 95 % CI [−66.9, −42.5] t ha^{-1} yr^{-1} for the below-canopy points (C) (Fig. 5 B). Overall, most sampling points (n = 73) indicated soil erosion rates with a mean value of −75.3 ± 28.3 t ha^{-1} yr^{-1} whereas soil deposition occurred in 10 points of the study area with a mean value of 33.7 ± 18.7 t ha^{-1} yr^{-1}. The interpolated $^{239+240}$Pu maps based on the inter-row (X) and below-canopy (C) points, show remarkable similarity (Fig. 5A and B). However, the catchment exhibits higher soil erosion rates when using the interpolated $^{239+240}$Pu map derived from inter-row (X) points. The highest soil erosion rates, locally greater than 100 t ha^{-1}yr^{-1}, were found in areas of concentrated runoff related to the gully (Fig. 1), in areas with steeper slopes and near the field boundaries (Fig. 5 A and B). The catchment experiences deposition rates ranging from 17.7 to 71.7 t ha^{-1} yr^{-1}, with the highest values occurring along the thalweg (Fig. 5 A and B). In the interpolated

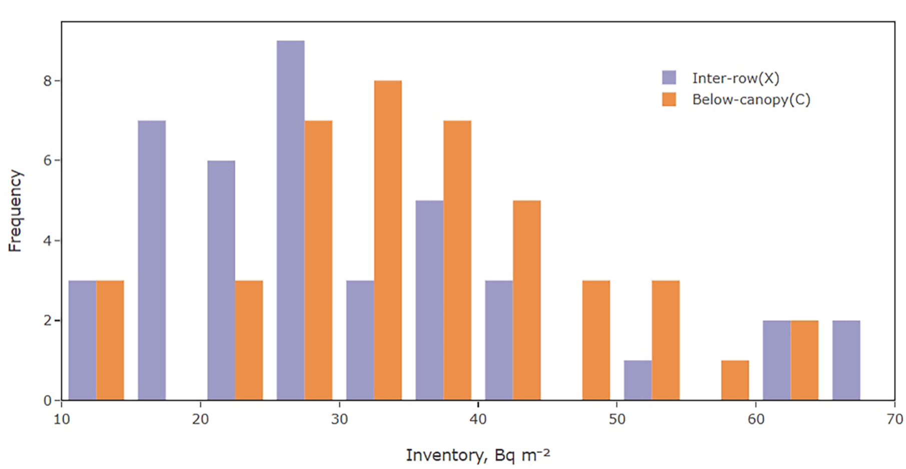

Fig. 4. Histograms comparing the $^{239+240}$Pu inventories of inter-row (X) and below-canopy (C) points.

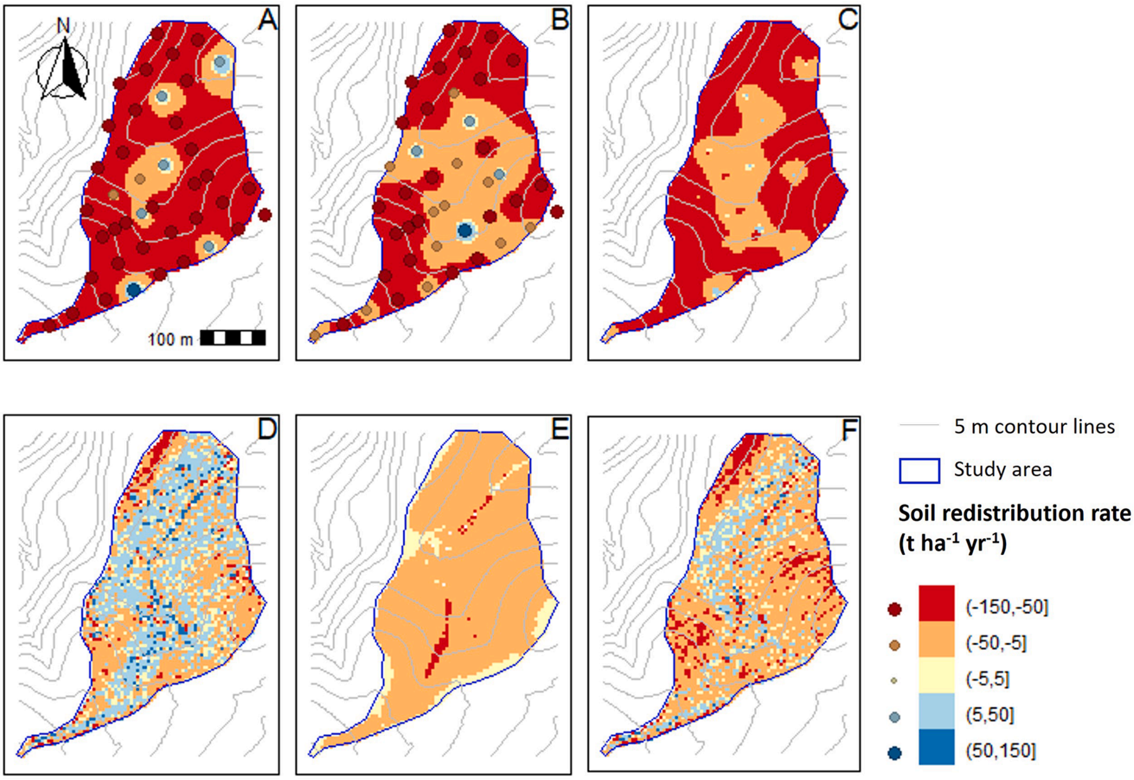

Fig. 5. Maps of estimated soil redistribution (net soil loss) rates. A. Soil redistribution derived from $^{239+240}$Pu at inter-row (X) points and the interpolated map; B. Soil redistribution derived from $^{239+240}$Pu at below-canopy (C) points and the interpolated map; C. Interpolated soil redistribution based on all $^{239+240}$Pu (X and C) point estimates; D. Modelled tillage erosion with a tillage transport coefficient (k_{till}) of 600 kg m^{-1}; E. Modelled water erosion (k_{tc}: 2000 m); F. Modelled total erosion. 5 m contour lines (lines in grey). Study area perimeter in blue.

$^{239+240}$Pu maps, the deposition is not continuous but rather localized at the inter-row (X) and below-canopy (C) points (Fig. 5A and B). The average net soil erosion for the catchment, calculated from the interpolated $^{239+240}$Pu map (Fig. 5C), is -59.4 ± 20 t ha^{-1}yr^{-1}. This value is considerably higher compared to the average measured sediment yield data for the period 2006–2011, 16.1 t ha^{-1} yr^{-1} (Gómez et al., 2014b). Three reasons can be put forward to explain this high difference. Firstly, the flume observations only represent water erosion, while the loss rates estimated from Pu isotopes represent total erosion, including tillage erosion. The latter can be quite significant in Mediterranean areas with values up to -57.4 t ha^{-1} yr^{-1} (De Alba and Van Oost, 2005). Second, human-induced land leveling operations during the implantation of the orchard, are not accounted for in the flume-based measurements.

Lastly, a third factor contributing to this discrepancy is the disparity in time scales represented by the Pu-based estimations period (~50 years) and the sediment yield measurements (5 years). It must be noted that the measurement period (2006–2011), covered a diverse spectrum of conditions, including an exceptionally dry year with a sediment yield of -1.45 t ha^{-1} yr^{-1} in 2008–2009 and an exceptionally wet year with a sediment yield of -52 t ha^{-1} yr^{-1} in 2009–2010 (Gómez et al., 2014b). While this is appropriate for model calibration purposes, these exceptional values greatly influence the 5-year average and can partially explain this difference with the Pu-based longer-term average, which is considerably less influenced by exceptional years (González-Hidalgo et al., 2009).

The average net soil erosion obtained, -59.4 t ha^{-1}yr^{-1}, has a better agreement with values obtained in catchments presenting similar characteristics in the province, in particular a similar average slope gradient. Vanwalleghem et al. (2010) estimated historical net soil losses, in representative olive orchards in the province of Córdoba, measuring tree mound heights. According to their findings, the soil loss rate was -66 t ha^{-1} yr^{-1} at Bujalance, with an average slope of 10 %, and -105 t ha^{-1} yr^{-1} and -61 t ha^{-1} yr^{-1} at two sites in Córdoba with an average slope of 13 %.

Previously, the output derived from the use of MODERN with Pu isotopes has been systematically compared to the results obtained by other models such as the Inventory method, the proportional model, the profile distribution model, or the diffusion and migration model (Arata et al.,2016a). Attending to the shape of the reference profile and the soil management (ploughed), the results of soil erosion or deposition rates obtained by using MODERN in the 60 cm depth sampling sites have been compared with those obtained by the proportional model (Walling et al., 2002), where the redistribution rates are calculated according to:

$$E = 10\frac{\rho dX}{100tP} \tag{5}$$

where E is the soil redistribution rate (t ha^{-1} yr^{-1}), d = 0.5 m the depth of the plough layer, ρ the bulk density (kg m^{-3}), X the percentage reduction or increment in total $^{239+240}$Pu inventory (%), t the time elapsed since the accumulation of plutonium (yr, same than for MODERN) and P a dimensionless particle size correction factor which is usually less than 1.0 and following (Zhang et al., 2015a) has been chosen as 0.65 as a commitment solution. As can be seen in Fig. 6, there is a good correlation obtained by the use of both models (adjusted R^2 = 0.98514), although there are certain sources of systematic bias that should be explained.

The independent term (b = 19.18 ± 0.90 t ha^{-1} yr^{-1}) shows a systematic bias (overestimation) of the calculated erosion rates by using MODERN when the calculated values are low. Furthermore, the slope is not 1.0 but 0.766 ± 0.011, showing an apparent underestimation of the values in the case of MODERN regarding the proportional model when the erosion rates are high. This finding is not surprising bearing in mind that according to Walling et al. (2002), the estimates provided by the proportional model are likely to underestimate the rates of soil loss

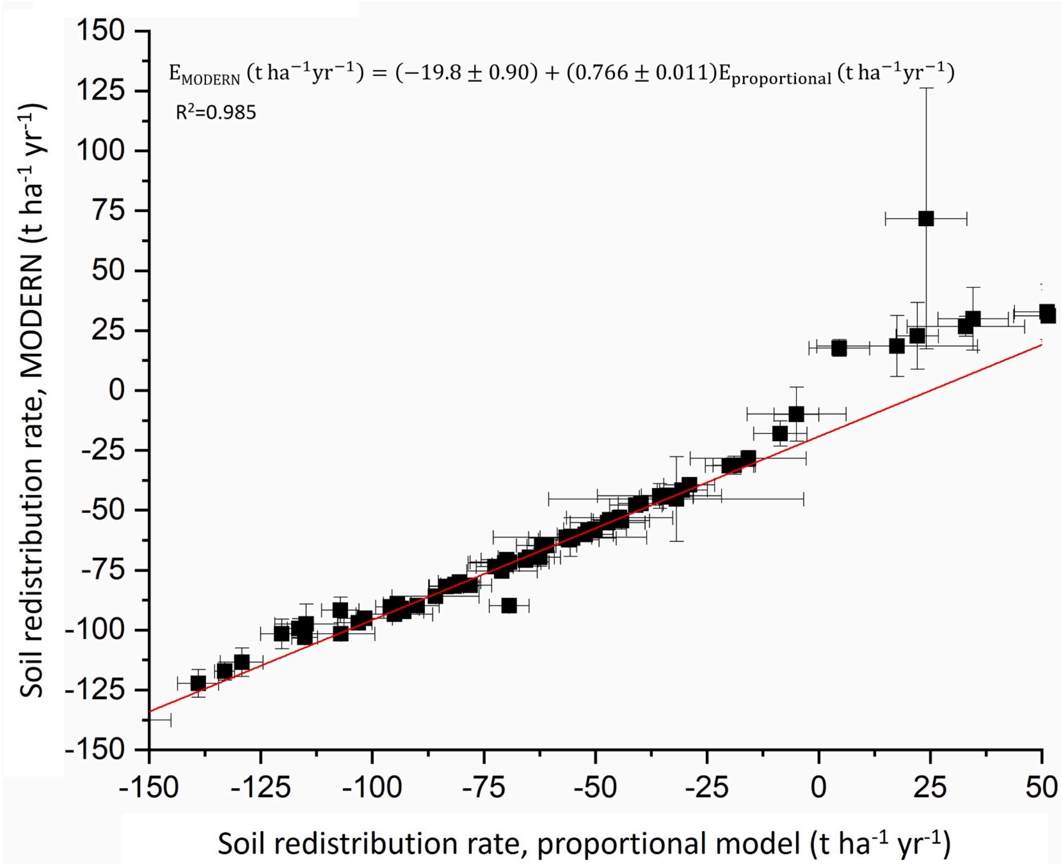

Fig. 6. Comparison of the soil redistribution rates obtained by MODERN and the proportional model for the 60 cm depth sampling points. Please see the text for details.

owing to the considered assumptions. In any case, what the data comparison reveals is that the calculated values fall within a similar order of magnitude as those provided by MODERN. This offers the relative advantage of preventing an oversimplification of the erosion and deposition scenario.

3.2. $^{239+240}$Pu soil redistribution rates related to topographical features

The results indicate weak correlations of $^{239+240}$Pu-based soil redistribution rates with topographical features (see Table 2 in the Supplementary Material). Only the slope gradient shows a significant but weak correlation. In contrast, different authors found a significant relationship between these variables and soil redistribution rates; Zhang et al. (2015b) found that the relationship between slope gradient and soil erosion rate follows a quadratic curve but not a linear fashion in their study of a catchment in the Loess Plateau region of China. Pennock and De Jong (1987) however, pointed out that the susceptibility of landform elements to erosion differs depending on the profile and plan curvature and slope gradient of a hillslope. Ritchie and McHenry (1990) found that erosion and deposition rates measured using the spatial distribution of ^{137}Cs were related to slope gradient, shape, and length. Flat areas at the top of slopes showed little soil loss while flat areas at the base of slopes and concave slopes in fields often showed deposition. Indeed, Panagos et al. (2015a) highlighted that the LS factor has the greatest impact on soil loss at the European level. The absence of correlation in this catchment is therefore surprising but might be attributed to the important land leveling during the implementation of the orchard and to the uncertainty associated with the Pu-based estimates. These results do not provide insights into the relative influence of water and tillage erosion on the total net erosion.

3.3. WaTEM/SEDEM model calibration

WaTEM/SEDEM calibration resulted in an optimal value for k_{tc},m of 2000 m according to the NS efficiency (Fig. 7). The NSE value at this point is 0.53. Even when there is not a universally agreed-upon value for the NSE that is considered satisfactory, an NSE value equal to or higher than 0.5 is often considered acceptable for many applications (Ritter and Muñoz-Carpena, 2013). As mentioned above, k_{tc}, which is dependent on both the land use and the DEM resolution, needs to be calibrated for each application of the model. In the same study area, Gómez et al. (2023) calibrated an optimum $k_{tc} = 175$ m using a 1 m resolution DEM. However, Quijano et al. (2016), in another Mediterranean agroecosystem, calibrated an optimum $k_{tc} = 1.28$ m using a 2.5 m DEM resolution. In addition, the calibration of the WaTEM/SEDEM model in these mentioned papers follows two different approaches: sediment yield data and soil redistribution rates derived from ^{137}Cs, respectively.

3.4. WATEM/SEDEM soil redistribution rates

The use of FRN-based soil erosion estimates does not allow differentiation between soil erosion caused by water erosion or due to tillage practices. For this purpose, we need a soil erosion model capable of simulating both processes, such as the WaTEM/SEDEM model. Fig. 5 F shows the spatial distribution of soil redistribution rates predicted by WaTEM/SEDEM for the study catchment with a mean value of -20 ± 29.0 t ha^{-1} yr^{-1}. The model estimates soil erosion across 78.5 % of the catchment, with a mean value of -30.2 ± 21.2 t ha^{-1} yr^{-1} whereas soil deposition occurred in the remaining 21.5 % of the catchment, with a mean value of 18.4 ± 21.3 t ha^{-1} yr^{-1}. The interpolated $^{239+240}$Pu map (Fig. 5C) reflects this trend, with 99.4 % of the catchment exhibiting soil

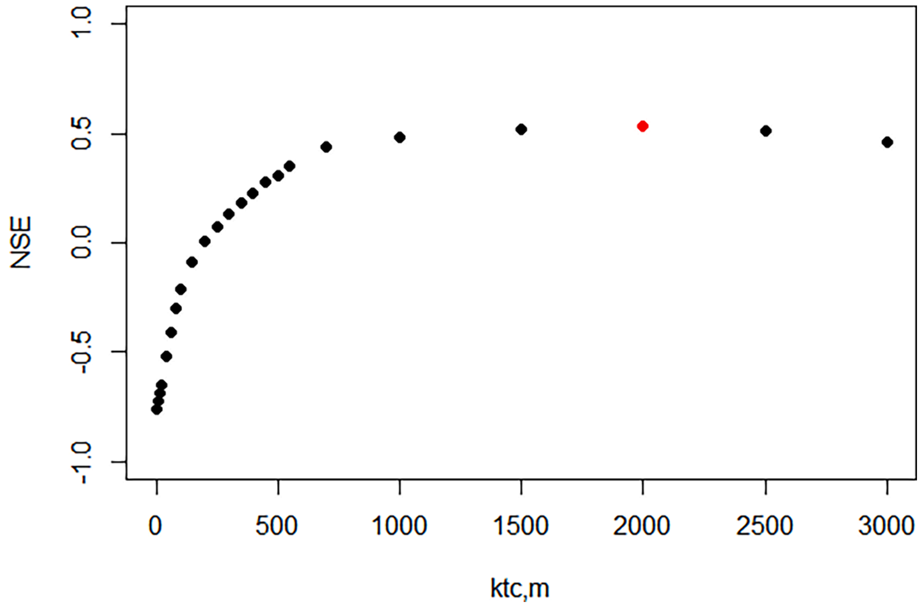

Fig. 7. WaTEM/SEDEM model transport capacity coefficient (k_{tc}, m) calibration curve for the study catchment. The optimum k_{tc}, m value, considering the Nash-Sutcliffe model efficiency (NSE) is 2000 m (dot in red).

erosion and only 0.6 % showing deposition.

Fig. 5 D and E illustrate the long-term soil erosion modeling of tillage and water erosion in the study catchment individually. Fig. 5 D shows that the majority of sediment deposition from slopes is attributed to tillage erosion, with a mean net erosion value equal to -0.7 ± 25.0 t ha^{-1} yr^{-1}. The water erosion map (Fig. 5 E) shows that the majority of the catchment exhibits high soil erosion rates, with areas of very high erosion in the thalweg where runoff is concentrated, with a mean net erosion value equal to -19 ± 11.6 t ha^{-1} yr^{-1}.

3.5. Results comparison and uncertainty reduction guidance

The comparison between WaTEM/SEDEM and the interpolated $^{239+240}$Pu map showed a poor correlation (Fig. 8). This can be attributed to the influence of the land leveling process and to the different sources of uncertainty that can be attributed to both methods (Bacchi et al., 2003; Belyaev et al., 2005; He and Walling, 2003; Lacoste et al., 2014; Warren et al., 2005). Li et al. (2007) observed discrepancies between ^{137}Cs-based estimates and model simulations in a Canadian catchment and claimed they were likely caused by the lack of data about the historical use of heavier tillage implements, and the low accuracy of historic climate data. Similarly, Quijano et al. (2016) attributed the lower performance of the WaTEM/SEDEM model in their study site in north-east Spain, to topographic changes in agricultural fields that were not directly related to water and tillage erosion. In our catchment of study, land leveling during the implantation of the orchard, consisting of ridges created along the tree lines to improve root aeration and disease management, most likely had an important impact on soil redistribution and

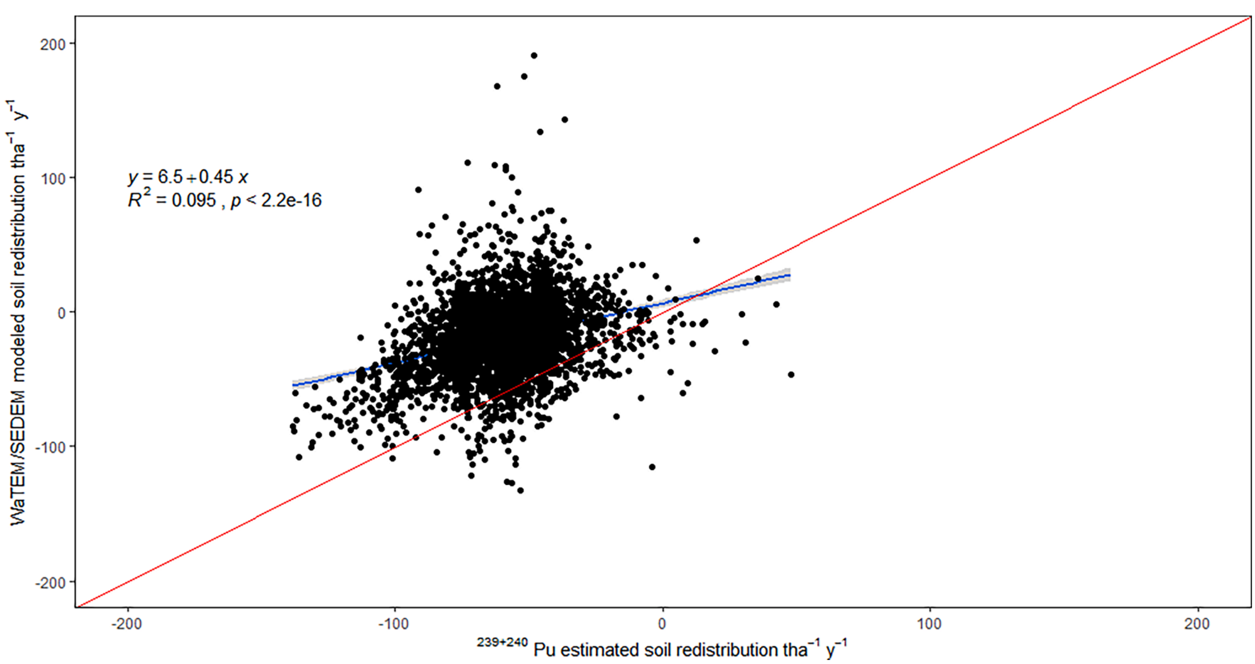

Fig. 8. Comparison between soil redistribution rates (t ha^{-1} yr^{-1}) modelled with WaTEM/SEDEM model and interpolated $^{239+240}$Pu map (line 1:1, in Red).

potentially be reflected in FRN-inventories (Bacchi et al., 2003; Lacoste et al., 2014; Quine, 1994) but not in the WaTEM/SEDEM simulations. The additional soil erosion at inter-row points due to this land leveling is estimated at -16 t ha^{-1} yr^{-1}. Nonetheless, adjusting the soil redistribution $^{239+240}$Pu-based point estimates, accounting for this estimated erosion overestimation or underestimation because of land leveling (Fig. 2), and comparing with WaTEM/SEDEM results does not yield markedly different results ($R^2 = 0.13$; p-value $= 0.0014$) from the current results ($R^2 = 0.095$; p-value $< 2.2 \bullet 10^{-16}$; Fig. 8). To reduce the uncertainty associated with this process we need detailed records of the process, with quantitative information on the volume of soil removed from the tree lanes to form the ridges. However, this information was not available in the study area. Ideally, this type of uncertainty can be reduced by the selection of catchments of study with a simple and well-documented land management history, especially those without changes in land use since the 1960s and without anthropogenic and drastic, processes that are challenging to quantify and simulate.

Another important anthropogenic source of uncertainty is the mechanized filling of rills in specific areas of the catchment which is a common practice in intensive olive orchards in South Spain. To our knowledge, no soil erosion model can simulate and quantify spatially targeted tillage practices. With FRN-based methods, we could increase the density of sampling points to evaluate the soil distribution in these specific areas of the catchment. However, due to the regular filling of rills or ephemeral gullies, we cannot identify their locations in the field. For this purpose, we can utilize model simulations, specifically the map of simulated net soil loss in the catchment. This map, which does not account for the rill-filling process, allows us to identify areas of concentration of high soil loss rates, which are more likely to develop rills or ephemeral gullies. In these identified areas, we can adjust the sampling strategy to accurately represent small-scale variations in FRN inventories. For instance, in these areas, we can increase the sampling density to measure FRN inventories at both points where the development of rills is more likely according to model simulations, and points at adjacent areas where the soil has been displaced to fill the rills. The differences between the simulated and the FRN-based soil loss rates would then reflect the effect of the rill filling process and provide an estimation of the volume of soil displaced by this process. It must be noted that while ephemeral gully or rill filling is a common practice, permanent gully filling is not allowed in the region of study.

Another potential source of uncertainty arises from the fact that WaTEM/SEDEM calibration was based on sediment yield measurements at the outlet of the catchment, which includes contributions from gully erosion. However, WaTEM/SEDEM does not simulate gully erosion. If the gully erosion contribution was significant during the calibration period (2006–2011), WaTEM/SEDEM may tend to overestimate hillslope erosion rates. Despite this, we observe an underestimation with respect to the $^{239+240}$Pu estimates, suggesting that the gully erosion contribution may not be significant. WaTEM/SEDEM calibration could be improved by extending the calibration period, however, setting up and maintaining sediment monitoring equipment at the outlet of catchments is logistically challenging and the financial resources required for long-term operation are a limiting factor. It must be noted that in this study the calibration period is still longer compared to other studies (Table 2). Another way to improve model calibration is to use spatial estimates of erosion–deposition rates, such as soil truncation measurements (Zhidkin et al., 2023), net soil erosion estimates based on tree mound measurements (Vanwalleghem et al., 2010), or FRN-based estimates. However, we always must use this data with caution and acknowledge their associated uncertainties, both inherent to the method itself and specific to the conditions of the study area. It must be noted that during the calibration of the WaTEM/SEDEM model, changes in the parameter k_{tc} only affected the model results in a small area of the catchment, the lower zone closer to the outlet. This indicates that, for calibration purposes, only spatial estimates of erosion–deposition rates in this specific area would be valuable. Therefore, for sampling strategies based on a grid covering the entire catchment, only a small part of the total number of spatial estimates of erosion–deposition rates would be considered during the model calibration. This opens the possibility of enhancing model calibration through the optimization of the sampling strategy, focusing efforts on areas where the calibrated parameters have a discernible impact on model results.

The third reason for the observed discrepancies can be related to the uncertainty in the $^{239+240}$Pu estimates. This method, and FRN-based methods in general, rely on several assumptions that can introduce uncertainties into the results. These include assumptions of a uniform spatial distribution, strong binding to soil particles, negligible plant uptake, minimal leaching by water, no chemical migration, and movement solely through physical processes. Additionally, the reliability of the results is influenced by the appropriateness of the chosen soil sampling design. The conversion models of FRN inventories into erosion rates, such as MODERN, are also a source of substantial uncertainty. In this study, we consider $^{239+240}$Pu-based estimates as highly uncertain since the vertical profile of the $^{239+240}$Pu inventories both in the sampling sites and in the reference site profile have been disturbed by tillage practices. It must be noted that no undisturbed profiles could be found in this area. The basic idea behind this MODERN is the comparison of the depth profile of the reference site with the total inventory of a sampling site. When comparing an undisturbed reference site with a ploughed site, MODERN assumes that the vertical distribution of FRN at the ploughed site is the same as in the reference site. While this assumption already introduces uncertainty, the level of uncertainty escalates when the reference site has also been ploughed (Fig. 3). In such cases, MODERN might fail to converge, presenting multiple possible solutions. The large uncertainty associated with $^{239+240}$Pu-based estimates indicates the need for further research in future studies. To reduce this uncertainty, we advocate for a more careful selection of the study catchment and reference site that ideally have not undergone ploughing, land leveling, and rill filling, or at the very least, finding a nearby undisturbed reference site.

Additionally, uncertainty arises from the performance of the interpolation method. When transforming point data, such as soil loss estimates, into a map through spatial interpolation, it is important to consider and address the uncertainty associated with this process. A way to reduce this source of uncertainty is to perform cross-validation, by withholding a subset of your data points or by sampling additional points and using the interpolation method to estimate their values. Then compare the estimated values with the actual values to assess the accuracy and reliability of different interpolation methods and select the one with better results.

These uncertainties need to be considered separately and reduced when possible. Table 3 summarizes the possible sources of uncertainty causing the poor relation between WaTEM/SEDEM and $^{239+240}$Pu soil redistribution rates and the proposed solutions to reduce these

Table 3
Sources of uncertainty and proposed solutions to improve the poor relation between WaTEM/SEDEM and interpolated 239+240Pu soil redistribution rates.

Sources of uncertainty	Solutions
Land leveling	Select a study area with a simpler land use and management history. If available, use detailed records of the process.
Rill filling	Identification of rill filling areas using model simulations and increase of the density of spatial sampling points in this area.
WaTEM/SEDEM calibration	Spatially distributed calibration procedures by using reliable spatial soil loss estimates. Sensitivity analysis of k_{tc} to optimize soil sampling strategy.
Model MODERN assumptions	Study area where the soil has not been ploughed. Reference site in an undisturbed zone.
Spatial interpolation of FRN-based point estimates	Cross-validation to compare different interpolation methods.

uncertainties.

3.6. Soil security dimensions: How long till we run out of soil?

The effect of the intense erosion rates on the evolution of a typical soil erosion profile in the study catchment is shown in Fig. 9. This soil profile has an A, B, BC, and C horizon (Table 1 Supplementary Material). The C horizon starts at 110 cm and is very weakly developed, with a massive structure. This implies that once soil erosion reaches this layer, an important drop in water availability and crop productivity can be expected. In 2010, when the soil pit was analyzed, the soil profile depth was 2.0 m. The soil type is a relatively fertile Vertisol. Next, the backward reconstruction of the soil profile was performed until 1963, considering two scenarios: using the mean soil erosion rates $^{239+240}$Pu estimates at erosion points, −75.3 t ha^{-1} yr^{-1}, (Fig. 9 A) and WaTEM/SEDEM modelled, −30.2 t ha^{-1} yr^{-1} (Fig. 9 B). By the year 2023, between 0.30 and 0.12 m of topsoil has been lost, using the $^{239+240}$Pu estimates and modelled erosion rates respectively. This implies that in the first case, the complete A horizon has been already lost, and in the second case it has been reduced by half, but the olive groves are still being grown. Land use changes are monitored by the concepts proposed by Huang et al. (2018): Phenosoil and Genosoil. In Phenosoils or domesticated cropping soils long-term soil management jeopardizes soil security, exceeding the capability of soils to recover their original conditions, i.e., its reference state or genosoil. Soil condition or soil status might be inferred from $^{239+240}$Pu estimated soil redistribution rates and WaTEM/SEDEM modelled soil redistribution rates. In the study zone, the poor management of soils influenced its capability and might interfere with affecting one of their main functions: food production (Bouma et al., 2017). Due to its high resistance to drought and ability to grow in low-quality soils, olive trees are suitable for growing on land that is unsuitable for many other crops. However, olive productivity might be affected as soil conditions worsen further or as drought events become more frequent (Molina de la Rosa, 2010). Based on $^{239+240}$Pu estimates of soil redistribution rates, soil loss would have been 0.70 m and 1.20 m by 2100 and 2200, respectively, since 1963 (Fig. 9 A). For the scenario considering WaTEM/SEDEM soil redistribution rates, soil erosion would have been 0.30 m and 0.50 m by 2100 and 2200, respectively, since 1963 (Fig. 9 B). Despite their discrepancies, both methods yield similar conclusions and indicate that the soil will have lost the A and B horizons, which are the most fertile layers, and the soil's capability to provide different functions will be significantly degraded jeopardizing the viability of the olive orchard.

To manage the soil according to its potential, individuals must be connected to the soil through the knowledge of its resources (Bouma et al., 2017). On this matter, concern about soil erosion in olive orchards by farmers and stakeholders is not new. Despite this, farmers can be reluctant to change their management practices for different reasons from profits to their concern for the environment (Ogieriakhi and Woodward, 2022). Sustainable soil management requires the codification of specific policies. Soil sustainability concerns are included in the EU soil strategy for 2030 to improve soil health by 2050 (European Commission, 2021) and in the Common Agricultural Policy strategic plans for 2023–2027 (CAP, 2022). In the strategy, the Commission committed to adopting a new Soil Health Law to protect soils. In this way, the development of a suitable and simple indicator that recognizes soil capital value might encourage practices that are more sustainable and raise awareness about present and future soil loss issues.

4. Conclusions

In this study, we evaluate the potential of using two methods $^{239+240}$Pu and the WaTEM/SEDEM model for estimating soil redistribution rates in a Mediterranean olive orchard and evaluate the contribution of water and tillage erosion. For this purpose, we compare the results obtained from the conversion of $^{239+240}$Pu into soil redistribution rates using MODERN and the results obtained from the WaTEM/SEDEM model calibrated with sediment yield data measured at the catchment outlet. We also identify possible sources of uncertainty that can explain the discrepancies in the results and provide guiding to reduce uncertainty. Moreover, we evaluate the correlation between the interpolated $^{239+240}$Pu map with topographical features of the catchment potentially related to water and tillage erosion.

Results show important discrepancies between $^{239+240}$Pu-based and WaTEM/SEDEM estimates. In this sense, these results indicate that both methods are considerably affected by several sources of uncertainty, both inherent to the methods themselves and related to the specific conditions of the study area. The latter are mainly related to anthropogenic changes in the soil surface related to soil tillage and rill filling practices and an important past land leveling effect performed during the implantation of the olive orchard in the catchment of study. This study demonstrates the potential advantages of combining FRN-based estimates and model simulations to optimize the sampling strategy, in particular, to improve model calibration and to evaluate the impact of rill-filling practices. Counterintuitively, $^{239+240}$Pu estimated soil redistribution rates showed a weak correlation with the different topographic features and hence, no insights about the soil erosion process that contributes most to total erosion. Only based on the mean values obtained using WaTEM/SEDEM, water erosion appears to be the predominant process. Despite the discrepancies, the estimated soil redistribution rates by both methods, Pu and WaTEM/SEDEM, convey a similar overarching message: soil security is highly threatened in the next decades. By 2100

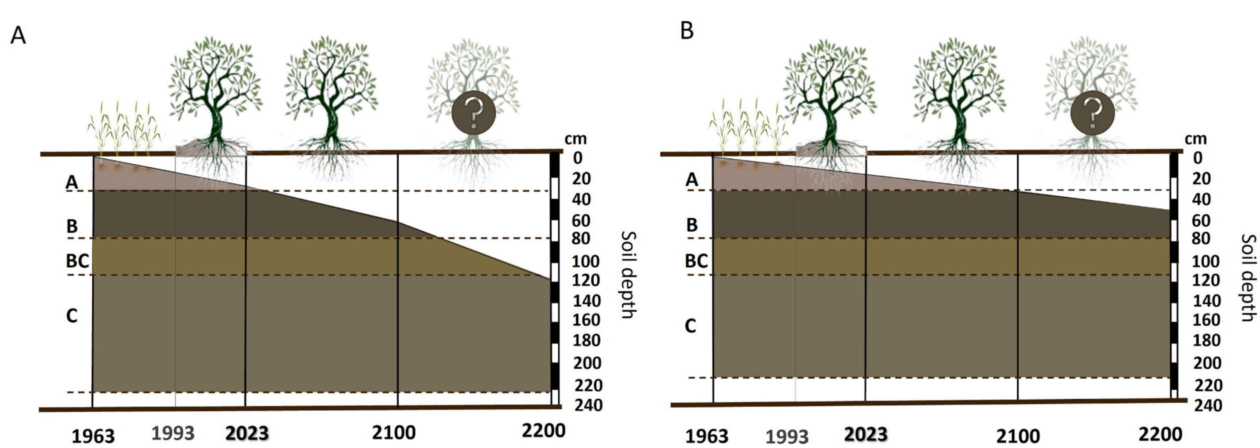

Fig. 9. Evolution of soil profile between 1963 and 2200 on an eroding position for the mean A. $^{239+240}$Pu and B. WaTEM/SEDEM soil redistribution rate. The top of the figure represents the change in land use from cereal to olive grove in 1993 and the uncertainty about the viability of the olive orchard beyond 2100.

and 2200, the soil will have lost the A and B horizons, respectively, and its ability to provide necessary conditions for olive production will be significantly diminished even jeopardizing the viability of the olive orchard.

The results and guidance from this study highlight the need for caution when selecting the study area and when estimating soil redistribution rates using FRN-based or modelling methods. Both FRN and modelling methods have uncertainties that need to be evaluated and when possible reduced. FRN-based estimates should not be assumed accurate for calibration or validation before the associated uncertainties are evaluated. Ideally, by combining the results of two uncertain but independent approaches, we can enhance the credibility of the study findings and conclusions, particularly when both methods yield similar results. Nevertheless, this study highlights how discrepancies between the approaches not only provide valuable insights but also shed light on the limitations and sources of uncertainty associated with each approach.

CRediT authorship contribution statement

Vanesa García-Gamero: Writing – review & editing, Writing – original draft, Visualization, Investigation, Formal analysis, Data curation. **J.L. Mas:** Writing – review & editing, Validation, Methodology, Formal analysis, Data curation, Conceptualization. **Andrés Peñuela:** Writing – review & editing, Validation, Methodology, Investigation, Conceptualization. **Santiago Hurtado:** Writing – review & editing, Conceptualization. **Adolfo Peña:** Writing – review & editing, Validation, Conceptualization. **Tom Vanwalleghem:** Writing – review & editing, Validation, Supervision, Project administration, Methodology, Funding acquisition, Conceptualization.

Declaration of competing interest

The authors declare that they have no known competing financial interests or personal relationships that could have appeared to influence the work reported in this paper.

Data availability

Data will be made available on request.

Acknowledgments

This work was supported by the project "Quantifying the impact of soil erosion and climate change on soil security by using alternative fallout radionuclides" (PID2019-109924RB-I00/AEI/10.13039/501100011033) funded by the Spanish Ministry of Science, Innovation and Universities co-financed by the EU. García-Gamero, Peñuela, and Vanwalleghem acknowledge financial support from the Department of Agronomy, of the Spanish Ministry of Science and Innovation, the Spanish State Research Agency, through the Severo Ochoa and María de Maeztu Program for Centers and Units of Excellence in R&D (Ref. CEX2019-000968-M). Andres Peñuela is funded by the European Research Executive Agency (REA) under the HORIZON-MSCA-2021-PF-01 grant agreement 101062258. The authors thank Dr. José A. Gómez, Dr. Gema Guzmán, and Dr. Karl Vanderlinden who provided the soil samples analyzed in this study. The authors thank to University of Seville, Research, Technology, and Innovation Centre (CITIUS) for granting the use of their laboratories for sample preparation and the use of ICP-MS.

Appendix A. Supplementary material

Supplementary data to this article can be found online at https://doi.org/10.1016/j.catena.2024.108052.

References

Alatorre, L.C., Beguería, S., García-Ruiz, J.M., 2010. Regional scale modeling of hillslope sediment delivery: a case study in the Barasona Reservoir watershed (Spain) using WATEM/SEDEM. J. Hydrol. (Amst.) 391, 109–123. https://doi.org/10.1016/j.jhydrol.2010.07.010.

Alewell, C., Meusburger, K., Juretzko, G., Mabit, L., Ketterer, M.E., 2014. Suitability of 239+240Pu and 137Cs as tracers for soil erosion assessment in mountain grasslands. Chemosphere 103, 274–280. https://doi.org/10.1016/J.CHEMOSPHERE.2013.12.016.

Alewell, C., Pitois, A., Meusburger, K., Ketterer, M., Mabit, L., 2017. 239 + 240Pu from " contaminant " to soil erosion tracer : Where do we stand ? Earth Sci. Rev. 172, 107–123. https://doi.org/10.1016/j.earscirev.2017.07.009.

Arata, L., Alewell, C., Frenkel, E., A'Campo-Neuen, A., Iurian, A.R., Ketterer, M.E., Mabit, L., Meusburger, K., 2016a. Modelling Deposition and Erosion rates with RadioNuclides (MODERN) - Part 2: A comparison of different models to convert 239 +240Pu inventories into soil redistribution rates at unploughed sites. J. Environ. Radioact. 162–163, 97–106. https://doi.org/10.1016/J.JENVRAD.2016.05.009.

Arata, L., Meusburger, K., Frenkel, E., A'Campo-Neuen, A., Iurian, A.R., Ketterer, M.E., Mabit, L., Alewell, C., 2016b. Modelling Deposition and Erosion rates with RadioNuclides (MODERN) – Part 1: A new conversion model to derive soil redistribution rates from inventories of fallout radionuclides. J. Environ. Radioact. 162–163, 45–55. https://doi.org/10.1016/J.JENVRAD.2016.05.008.

Bacchi, O.O.S., Reichardt, K., Sparovek, G., 2003. Sediment spatial distribution evaluated by three methods and its relation to some soil properties. Soil Tillage Res. 69, 117–125. https://doi.org/10.1016/S0167-1987(02)00133-2.

Batista, P.V.G., Davies, J., Silva, M.L.N., Quinton, J.N., 2019. On the evaluation of soil erosion models: Are we doing enough? Earth Sci. Rev. 197, 102898 https://doi.org/10.1016/J.EARSCIREV.2019.102898.

Belyaev, V.R., Wallbrink, P.J., Golosov, V.N., Murray, A.S., Sidorchuk, A.Y., 2005. A comparison of methods for evaluating soil redistribution in the severely eroded Stavropol region, southern European Russia. Geomorphology 65, 173–193. https://doi.org/10.1016/J.GEOMORPH.2004.09.001.

Bouma, J., van Ittersum, M.K., Stoorvogel, J.J., Batjes, N.H., Droogers, P., Pulleman, M. M., 2017. Soil Capability: Exploring the Functional Potentials of Soils. pp. 27–44. doi: 10.1007/978-3-319-43394-3_3.

CAP, 2022. Common agricultural policy for 2023-2027 28 CAP strategic plans at a glance.

Daggupati, P., Pai, N., Ale, S., Douglas-Mankin, K.R., Zeckoski, R.W., Jeong, J., Parajuli, P.B., Saraswat, D., Youssef, M.A., 2015. A recommended calibration and validation strategy for hydrologic and water quality models. Trans. ASABE 58, 1705–1719. https://doi.org/10.13031/trans.58.10712.

De Alba, S., Van Oost, K., 2005. Erosión mecánica (tillage erosion) vs. erosión hídrica. In: II Simposion NACIONAL sobre control de la degradación de suelos.

Junta de Andalucía, 2022. Programa de desarrollo rural de andalucía 2014-2022 Subprograma temático del sector del olivar.

Durán, Z.V.H., Rodríquez Pleguezuelo, C.R., Arroyo Panadero, L., Martínez Raya, A., Francia Martínez, J.R., Cárceles Rodríguez, B., 2009. Soil conservation measures in rainfed olive orchards in south-eastern Spain: impacts of plant strips on soil water dynamics * 1. Pedosphere: Int. J. 19, 453–464. https://doi.org/10.1016/S1002-0160(09)60138-7.

European Commission, 2021. EU Soil Strategy for 2030. Brussels.

Gómez, J.A., Battany, M., Renschler, C.S., Fereres, E., 2003. Evaluating the impact of soil management on soil loss in olive orchards. Soil Use Manag. 19, 127–134. https://doi.org/10.1111/J.1475-2743.2003.TB00292.X.

Gómez, J.A., Sobrinho, T.A., Giráldez, J.V., Fereres, E., 2009. Soil management effects on runoff, erosion and soil properties in an olive grove of Southern Spain. Soil Tillage Res. 102, 5–13. https://doi.org/10.1016/j.still.2008.05.005.

Gómez, J.A., Infante-Amate, J., González De Molina, M., Vanwalleghem, T., Taguas, E.V., Lorite, I., 2014a. Olive cultivation, its impact on soil erosion and its progression into yield impacts in southern Spain in the past as a key to a future of increasing climate uncertainty. Agriculture 4, 170–198. https://doi.org/10.3390/agriculture4020170.

Gómez, J.A., Vanwalleghem, T., De Hoces, A., Taguas, E.V., 2014b. Hydrological and erosive response of a small catchment under olive cultivation in a vertic soil during a five-year period: Implications for sustainability. Agric. Ecosyst. Environ. 188, 229–244. https://doi.org/10.1016/j.agee.2014.02.032.

Gómez, J.A., Guzmán, G., Vanwalleghem, T., Vanderlinden, K., 2023. Spatial variability of soil organic carbon stock in an olive orchard at catchment scale in Southern Spain. Int. Soil Water Conserv. Res. https://doi.org/10.1016/J.ISWCR.2022.12.002.

Gómez-Limón, J.A., Picazo-Tadeo, A.J., Reig-Martínez, E., 2012. Eco-efficiency assessment of olive farms in Andalusia. Land Use Policy 29, 395–406. https://doi.org/10.1016/j.landusepol.2011.08.004.

González-Hidalgo, J.C., de Luis, M., Batalla, R.J., 2009. Effects of the largest daily events on total soil erosion by rainwater. An analysis of the usle database. Earth Surf. Proc. Land. 34, 2070–2077. https://doi.org/10.1002/ESP.1892.

Govers, G., Lobb, D.A., Quine, T.A., 1999. Tillage erosion and translocation: emergence of a new paradigm in soil erosion research. Soil Tillage Res. 51, 167–174.

Guillén, J., Baeza, A., Corbacho, J.A., Muñoz-Muñoz, J.G., 2015. Migration of (137)Cs, (90)Sr, and (239+240)Pu in Mediterranean forests: influence of bioavailability and association with organic acids in soil. J. Environ. Radioact. 144, 96–102. https://doi.org/10.1016/J.JENVRAD.2015.03.011.

He, Q., Walling, D.E., 2003. Testing distributed soil erosion and sediment delivery models using 137Cs measurements. Hydrol. Process. 17, 901–916. https://doi.org/10.1002/HYP.1169.

Hoo, W.T., Fifield, L.K., Tims, S.G., Fujioka, T., Mueller, N., 2011. Using fallout plutonium as a probe for erosion assessment. J. Environ. Radioact. 102, 937–942. https://doi.org/10.1016/J.JENVRAD.2010.06.010.

Huang, J., Mcbratney, A.B., Malone, B.P., Field, D.J., 2018. Mapping the transition from pre-European settlement to contemporary soil conditions in the Lower Hunter Valley, Australia. doi: 10.1016/j.geoderma.2018.05.016.

ICONA, I. para la C. de la N., 1988. Agresividad de la lluvia en España. Valores del factor R de la ecuación universal de pérdidas de suelo. Madríd.

Iurian, A.R., Olufemi Phaneuf, M., Mabit, L., 2015. Mobility and Bioavailability of Radionuclides in Soils. In: Walther, C., Gupta, D.K. (Eds.), Radionuclides in the Environment: Influence of Chemical Speciation and Plant Uptake on Radionuclide Migration. Springer, pp. 1–273. https://doi.org/10.1007/978-3-319-22171-7.

Jordan, G., Van Rompaey, A., Szilassi, P., Csillag, G., Mannaerts, C., Woldai, T., 2005. Historical land use changes and their impact on sediment fluxes in the Balaton basin (Hungary). Agric. Ecosyst. Environ. 108, 119–133. https://doi.org/10.1016/j.agee.2005.01.013.

Ketterer, M.E., Watson, B.R., Matisoff, G., Wilson, C.G., 2002. Rapid dating of recent aquatic sediments using Pu activities and. Environ. Sci. Tech. 36 https://doi.org/10.1021/es010826g.

Ketterer, M.E., Hafer, K.M., Link, C.L., Kolwaite, D., Wilson, J., Mietelski, J.W., 2004. Resolving global versus local/regional Pu sources in the environment using sector ICP-MS. J. Anal. At. Spectrom 19, 241–245. https://doi.org/10.1039/B302903D.

Lacoste, M., Michot, D., Viaud, V., Evrard, O., Walter, C., 2014. Combining 137Cs measurements and a spatially distributed erosion model to assess soil redistribution in a hedgerow landscape in northwestern France (1960–2010). Catena (Amst.) 119, 78–89. https://doi.org/10.1016/J.CATENA.2014.03.004.

Lal, R., Tims, S.G., Fifield, L.K., Wasson, R.J., Howe, D., 2013. Applicability of 239Pu as a tracer for soil erosion in the wet-dry tropics of northern Australia. Nucl. Instrum. Methods Phys. Res. B 294, 577–583. https://doi.org/10.1016/J.NIMB.2012.07.041.

Li, S., Lobb, D.A., Lindstrom, M.J., Farenhorst, A., 2007. Tillage and water erosion on different landscapes in the northern North American Great Plains evaluated using 137Cs technique and soil erosion models. Catena (Amst.) 70, 493–505. https://doi.org/10.1016/j.catena.2006.12.003.

Lizaga Villuendas, I., Latorre, B., Gaspar, L., Navas, A., 2022. Effect of historical land-use change on soil erosion in a Mediterranean catchment by integrating 137Cs measurements and WaTEM/SEDEM model. Hydrol. Process. 36 https://doi.org/10.1002/HYP.14577.

Lobb, D.A., 2006. Tillage erosion: measurement techniques. Encycl. Soil Sci. https://doi.org/10.1081/E-ESS-120042771.

Luo, Y., Wang, H., Meersmans, J., Green, S.M., Quine, T.A., Feng, S., 2021. Modeling soil erosion between 1985 and 2014 in three watersheds on the carbonate-rock dominated Guizhou Plateau, SW China, using WaTEM/SEDEM. Prog. Phys. Geogr. 45, 53–81. https://doi.org/10.1177/0309133320961274.

Mabit, L., Chhem-Kieth, S., Toloza, A., Vanwalleghem, T., Bernard, C., Amate, J.I., González de Molina, M., Gómez, J.A., 2012. Radioisotopic and physicochemical background indicators to assess soil degradation affecting olive orchards in southern Spain. Agric. Ecosyst. Environ. 159, 70–80. https://doi.org/10.1016/J.AGEE.2012.06.014.

Mai, J., 2023. Ten strategies towards successful calibration of environmental models. J. Hydrol. (Amst.) 620, 129414. https://doi.org/10.1016/J.JHYDROL.2023.129414.

Martinez, C., Hancock, G.R., Kalma, J.D., 2009. Comparison of fallout radionuclide (caesium-137) and modelling approaches for the assessment of soil erosion rates for an uncultivated site in south-eastern Australia. doi: 10.1016/j.geoderma.2009.03.023.

McBratney, A., Field, D.J., Koch, A., 2014. The dimensions of soil security. Geoderma 213, 203–213. https://doi.org/10.1016/J.GEODERMA.2013.08.013.

Meusburger, K., Alewell, C., Konz, N., Schaub, M., 2014. The combined use of 137Cs and stable isotopes to evaluate soil redistribution in montainous grasslands, Switzerland. In: IAEA-TEDOC-1741 (Ed.), Guidelines for Using Fallout Radionuclides to Assess Erosion and Effectiveness of Soil Conservation Strategies. Vienna, pp. 181–202.

Meusburger, K., Mabit, L., Ketterer, M., Park, J.H., Sandor, T., Porto, P., Alewell, C., 2016. A multi-radionuclide approach to evaluate the suitability of 239 + 240Pu as soil erosion tracer. Sci. Total Environ. 566–567, 1489–1499. https://doi.org/10.1016/J.SCITOTENV.2016.06.035.

Ministerio de Agricultura Pesca y Alimentación, 2022. Estadística Anual De Superficies y Producciones de cultivos.

Molina de la Rosa, J.L., 2010. Agronomía y poda del olivar.

Nash, J.E., Sutcliffe, J.V., 1970. River flow forecasting through conceptual models part I - a discussion of principles. J. Hydrol. (Amst.) 10, 282–290. https://doi.org/10.1016/0022-1694(70)90255-6.

Ogieriakhi, M.O., Woodward, R.T., 2022. Understanding why farmers adopt soil conservation tillage: a systematic review. Soil Secur. https://doi.org/10.1016/j.soisec.2022.100077.

Panagos, P., Borrelli, P., Meusburger, K., 2015a. A New european slope length and steepness factor (LS-Factor) for modeling soil erosion by water. Geosciences (Basel) 5, 117–126. https://doi.org/10.3390/geosciences5020117.

Panagos, P., Borrelli, P., Meusburger, K., Alewell, C., Lugato, E., Montanarella, L., 2015b. Estimating the soil erosion cover-management factor at the European scale. Land Use Policy 48, 38–50. https://doi.org/10.1016/J.LANDUSEPOL.2015.05.021.

Panagos, P., Montanarella, L., Barbero, M., Schneegans, A., Aguglia, L., Jones, A., 2022. Soil priorities in the European Union. Geoderma Reg. 29 https://doi.org/10.1016/J.GEODRS.2022.E00510.

Parsons, A.J., Foster, I.D.L., 2011. What can we learn about soil erosion from the use of 137 Cs? doi: 10.1016/j.earscirev.2011.06.004.

Peeters, I., Van Oost, K., Govers, G., Verstraeten, G., Rommens, T., Poesen, J., 2008. The compatibility of erosion data at different temporal scales. Earth Planet. Sci. Lett. 265, 138–152. https://doi.org/10.1016/j.epsl.2007.09.040.

Pennock, D.J., De Jong, E., 1987. The influence of slope curvature on soil erosion and deposition in Hummock terrain. Soil Sci. 144.

Peñuela, A., Hurtado, S., García-Gamero, V., Mas, J.L., Ketterer, M.E., Vanwalleghem, T., Gómez, J.A., 2023. A comparison of 210 Pb xs, 137 Cs, and Pu isotopes as proxies of soil redistribution in South Spain under severe erosion conditions. J. Soil. Sediment. https://doi.org/10.1007/s11368-023-03560-5.

Percich, A., Husic, A., Ketterer, M.E., 2022. Plutonium isotopes : an effective tool for fluvial sediment sourcing in urbanized catchments. Geophys. Res. Lett. 49, 1–11. https://doi.org/10.1029/2021GL094497.

Porto, P., Walling, D.E., Callegari, G., Spada, C. La, 2010. Exploring the relationship between sediment and fallout radionuclide output for two small Calabrian catchments.

Porto, P., Walling, D., La Spada, C., 2013. Using caesium-137 measurements to establish. IAHS-AISH Proc. Rep. 362, 125–133.

Quijano, L., Beguería, S., Gaspar, L., Navas, A., 2016. Estimating erosion rates using 137Cs measurements and WATEM/SEDEM in a Mediterranean cultivated field. Catena (Amst.) 138, 38–51. https://doi.org/10.1016/J.CATENA.2015.11.009.

Quine, T., 1994. A comparison of the roles of tillage and water erosion in landform development and sediment export on agricultural land near Leuven, Belgium. In: IAHS Publications-Series of Proceedings and Reports-Intern Assoc Hydrological Sciences.

R Core Team, 2023. R: A Language and Environment for Statistical Computing. R Foundation for Statistical Computing.

Raab, G., Scarciglia, F., Norton, K., Dahms, D., Brandová, D., de Castro Portes, R., Christl, M., Ketterer, M.E., Ruppli, A., Egli, M., 2018. Denudation variability of the Sila Massif upland (Italy) from decades to millennia using 10Be and 239+240Pu. Land Degrad. Dev. 29, 3736–3752. https://doi.org/10.1002/LDR.3120.

Renard, K.G., Foster, G.R., Weesies, G.A., Porter, J.P., 1991. RUSLE Revised universal soil loss equation.

Ritchie, J.C., Mchenry, J.R., 1990. Application of radioactive fallout Cesium-137 for measuring soil erosion and sediment accumulation rates and patterns: a review. J. Environ. Qual. 19, 215–233.

Ritter, A., Muñoz-Carpena, R., 2013. Performance evaluation of hydrological models: statistical significance for reducing subjectivity in goodness-of-fit assessments. J. Hydrol.(Amst.) 480, 33–45. https://doi.org/10.1016/j.jhydrol.2012.12.004.

Schimmack, W., Auerswald, K., Bunzl, K., 2001. Can 239+240Pu replace 137Cs as an erosion tracer in agricultural landscapes contaminated with Chernobyl fallout? J. Environ. Radioact. 53, 41–57. https://doi.org/10.1016/S0265-931X(00)00117-X.

Schimmack, W., Auserwald, K., Bunzl, K., 2002. Estimation of soil erosion and deposition rates at an agricultural site in Bavaria, Germany, as derived from fallout radiocesium and plutonium as tracers. Naturwissenschaften 89, 43–46. https://doi.org/10.1007/s00114-001-0281-z.

Schoeneberger, P.J., Wysocki, D.A., Benham, E.C., Soil Survey Staff, 2012. Field Book for Describing and Sampling Soils; Version 3.0. Natural Resources Conservation Service, National Soil Survey Center, Lincoln, NE.

Soil survey staff, 2022. Keys to Soil Taxonomy. USDA Natural Resources Conservation Service 13th edition.

Vandaele, K., Poesen, J., 1995. Spatial and temporal patterns of soil erosion rates in an agricultural catchment, central Belgium. Catena (Amst.) 25, 213–226.

Vanwalleghem, T., Laguna, A., Giráldez, J.V., Jiménez-Hornero, F.J., 2010. Applying a simple methodology to assess historical soil erosion in olive orchards. Geomorphology 114, 294–302. https://doi.org/10.1016/J.GEOMORPH.2009.07.010.

Vanwalleghem, T., Amate, J.I., de Molina, M.G., Fernández, D.S., Gómez, J.A., 2011. Quantifying the effect of historical soil management on soil erosion rates in Mediterranean olive orchards. Agric. Ecosyst. Environ. 142, 341–351. https://doi.org/10.1016/J.AGEE.2011.06.003.

Verstraeten, G., Van Oost, K., Rompaey, A.V., Poesen, J., Govers, G., 2002. Evaluating an integrated approach to catchment management to reduce soil loss and sediment pollution through modelling. Soil Use Manag. 19, 386–394. https://doi.org/10.1079/SUM2002150.

Verstraeten, G., Prosser, I.P., Fogarty, P., 2007. Predicting the spatial patterns of hillslope sediment delivery to river channels in the Murrumbidgee catchment, Australia. J. Hydrol. (Amst.) 334, 440–454. https://doi.org/10.1016/J.JHYDROL.2006.10.025.

Walling, D.E., He, Q., 2002. Using 137Cs measurements to test distributed soil erosion and sediment delivery models. In: Summer, W., Walling, Desmond E. (Eds.), Modelling Erosion, Sediment Transport and Sediment Yield. UNESCO, Paris, pp. 243–264.

Walling, D.E., He, Q., Appleby, P.G., 2002. Handbook for the Assessment of Soil Erosion and Sedimentation Using Environmental Radionuclides, Handbook for the Assessment of Soil Erosion and Sedimentation Using Environmental Radionuclides. Springer Netherlands. doi: 10.1007/0-306-48054-9.

Walling, D.E., He, Q., 1998. Use of fallout 137Cs measurements for validating and calibrating soil erosion and sediment delivery models. Int. Assoc. Hydrol. Sci. Publ. 249, 267–278.

Walling, D.E., He, Q., Whelan, P.A., 2003. Using 137 Cs measurements to validate the application of the AGNPS and ANSWERS erosion and sediment yield models in two small Devon catchments. Soil Tillage Res. 69, 27–43.

Warren, S.D., Mitasova, H., Hohmann, M.G., Landsberger, S., Iskander, F.Y., Ruzycki, T. S., Senseman, G.M., 2005. Validation of a 3-D enhancement of the Universal Soil Loss Equation for prediction of soil erosion and sediment deposition. Catena (Amst.) 64, 281–296. https://doi.org/10.1016/J.CATENA.2005.08.010.

Wilken, F., Ketterer, M., Koszinski, S., Sommer, M., Fiener, P., 2020. Understanding the role of water and tillage erosion from 239+240Pu tracer measurements using inverse modelling. Soil 6, 549–564. https://doi.org/10.5194/soil-6-549-2020.

Xu, Y., Qiao, J., Hou, X., Pan, S., 2013. Plutonium in soils from Northeast China and its potential application for evaluation of soil erosion. Sci. Rep. https://doi.org/10.1038/srep03506.

Zhang, K., Pan, S., Xu, Y., Cao, L., Hao, Y., Wu, M., Xu, W., Ren, S., 2016. Using 239+240Pu atmospheric deposition and a simplified mass-balance model to re-estimate the soil erosion rate: a case study of Liaodong Bay in China. J. Radioanal. Nucl. Chem. 307, 599–604. https://doi.org/10.1007/S10967-015-4208-0/FIGURES/3.

Zhang, Z., Sheng, L., Yang, J., Chen, X.A., Kong, L., Wagan, B., 2015b. Effects of land use and slope gradient on soil erosion in a red soil hilly watershed of southern China. Sustainability (Switzerland) 7, 14309–14325. https://doi.org/10.3390/su71014309.

Zhang, W., Xing, S., Hou, X., 2019. Evaluation of soil erosion and ecological rehabilitation in Loess Plateau region in Northwest China using plutonium isotopes. Soil Tillage Res. 191, 162–170. https://doi.org/10.1016/j.still.2019.04.004.

Zhang, X.C., Zhang, G.H., Wei, X., Guan, Y.H., 2015a. Evaluation of Cesium-137 conversion models and parameter sensitivity for erosion estimation. J. Environ. Qual. 44, 789–802. https://doi.org/10.2134/JEQ2014.09.0371.

Zheng, F., Maier, H.R., Wu, W., Dandy, G.C., Gupta, H.V., Zhang, T., 2018. On lack of robustness in hydrological model development due to absence of guidelines for selecting calibration and evaluation data: demonstration for data-driven models. Water Resour. Res. 54, 1013–1030. https://doi.org/10.1002/2017WR021470.

Zhidkin, A., Gennadiev, A., Fomicheva, D., Shamshurina, E., Golosov, V., Dokuchaev, V. V., 2023. Soil erosion models verification in a small catchment for different time windows with changing cropland boundary. Geoderma 430, 116322. https://doi.org/10.1016/j.geoderma.2022.116322.

Zollinger, B., Alewell, C., Kneisel, C., Meusburger, K., Brandová, D., Kubik, P., Schaller, M., Ketterer, M., Egli, M., 2015. The effect of permafrost on time-split soil erosion using radionuclides (137Cs, 239 + 240Pu, meteoric 10Be) and stable isotopes (δ13C) in the eastern Swiss Alps. J. Soils Sediments 15, 1400–1419. https://doi.org/10.1007/S11368-014-0881-9/FIGURES/6.